An analysis of the mean stress effect on fretting fatigue of Al 7050-T7451

Fábio Comes de Castro, fabiocastro@unb.br
Allisson Ribeiro Figueiredo, allisson.go@gmail.com
Bernardo Rodrigues Pereira, brodpereira@gmail.com
José Alexander Araújo, alex07@unb.br
Universidade Federal de Brasília – Departamento de Engenharia Mecânica, Brasília-DF, CEP 70910-900, Brasil

Abstract. *This paper presents an assessment of the mean stress effect on fretting fatigue of an aluminium alloy 7050-T7451. Experimental data were obtained from a cylinder-flat contact configuration under partial slip condition. All test parameters were kept constant except the mean bulk stress, which varied from a tensile to a compressive value. A threshold compressive mean stress was found below which tests ran out. For these tests, arrested cracks were observed. Two fretting fatigue endurance models are proposed and compared: a non-local multiaxial fatigue model and a crack arrest model. The non-local fatigue model correctly predicted crack initiation in all tests. Nevertheless, it predicted complete failure of the run out tests. The crack arrest model was able to predict both run out tests as well as complete failure.*

Keywords: fretting fatigue, crack self-arrest, mean stress effect, aluminum alloy

1. INTRODUCTION

Fretting is the minute oscillatory relative tangential displacement between contacting surfaces, typically having amplitudes of the order of microns (Hills and Nowell, 1994). The fretting process — which may also involve heat generation, oxidation and other complex tribological phenomena — provide an aggressive environment which encourages premature initiation of microcracks. Whenever one of the contacting bodies is also subjected to time-varying loads, initiated cracks may propagate under a combination of contact and remote stresses, causing failure by fretting fatigue. This failure mode typically occurs in mechanically fastened assemblies such as dovetail joints in turbine engines, suspension clamp–conductor cable arrangements and orthopedic replacement implants (Araújo and Castro, 2009).

One main effect in fretting fatigue is the presence of high stress gradients beneath the contact surface. In this setting, fretting fatigue endurance may be associated not only with the non-initiation of a crack, but also with the arrest of an initiated crack. Recent models for fretting fatigue endurance have tried to incorporate this effect. Crack arrest models (Araújo and Nowell, 1999; Fouvry et al., 2008) estimate crack driving force with fracture mechanics parameters, and predict crack self-arrest if its value reaches a material threshold. Non-local stress-based fatigue models (Fouvry et al., 2002; Araújo et al., 2007) consider an average value over a representative volume of the stresses beneath the contact surface. Although these models were able to correctly predict the size effect observed in the fretting fatigue tests performed by Nowell (1988), their application to different geometries, materials and loading histories are still necessary for a more conclusive assessment.

The aim of this paper is to assess two fretting fatigue endurance models when one of the contacting bodies bears a mean bulk stress. The assessment was carried out with new fretting fatigue data obtained from an experimental program where all test parameters, except the mean bulk load, were kept constant. One of the models proposes the application of a multiaxial critical plane fatigue model at a critical distance from the contact surface (Araújo et al., 2007). The other one is a crack arrest model which assumes a mode I crack growth normal to the contact surface, and compares the crack tip stress intensity range with the threshold range for crack propagation as a criterion for crack self-arrest (Araújo and Nowell, 1999).

2. EXPERIMENTAL RESULTS

This section summarizes the plain and fretting fatigue tests conducted by the authors. The fretting pads and the specimens were machined from rolled plates made of an 7050 Al alloy in the T7451 condition provided by EMBRAER-LIEBHERR (ELEB). Tables 1 and 2 report its nominal chemical composition and mechanical properties.

Table 1. Nominal chemical composition of the Al alloy 7050-T7451 in weight (%).

Zn	Ti	Mg	Cu	Zr	Fe	Mn	Cr	Ni	Si
5.7-6.7	0.06	1.9-2.6	2.0-2.6	0.10-0.16	0.15	0.009	0.006	-	0.12

In order to characterize the plain uniaxial fatigue behavior of the aluminum alloy, S-N curves for two levels of mean stress (0 and 120 MPa) were obtained. Fatigue failure was defined as the complete fracture of the specimen, and run out was set at 10^7 cycles. A least-squares fit of the data using Basquin's law provided the following relationships between

Table 2. Mechanical properties of Al 7050-T7451.

Yield strength (MPa)	453.8 ± 2.8
Tensile strength (MPa)	513.3 ± 4.1
Elastic modulus (GPa)	73.4 ± 2.0
Elongation (%)	11.1 ± 0.6
Microhardness (HV)	153.6 ± 2.6
Poisson's coefficient	0.3

the stress amplitude and the number of cycles to failure: $\sigma_a = 839N^{-0.1083}$ under fully reversed loading and $\sigma_a = 658N^{-0.1156}$ under a mean stress of 120 MPa. From these results, the fatigue strength at 10^7 cycles under fully reversed loading was estimated as 146.4 MPa and under a mean stress of 120 MPa as 102.2 MPa.

The fretting fatigue tests involved a pair of cylindrical pads pressed against a flat dog-bone specimen. Figure 1 shows a scheme of the contact configuration and the loading program. First, a mean bulk load B_m was applied to the specimen. Next, the pads were clamped producing a static normal load P. A sinusoidal bulk loading $B_a \sin(\omega t)$ was then applied to the specimen which, due to the stiffness of the fretting device, also experienced a tangential loading $Q(t) = Q_a \sin(\omega t - \pi)$. Ten fretting fatigue tests were carried out in the partial slip regime, i.e. $Q_a < fP$ where f is the friction coefficient. These tests were conducted for six levels of mean bulk stress $\sigma_m = B_m/A$ from 15 MPa to -145 MPa, where A is the cross-sectional area of the specimen. Two specimens were tested at each mean stress level, except in the case of -92.7 MPa and -145 MPa where only one specimen was used. Fatigue failure was defined as the complete fracture of the specimen, and run out was set at 10^7 cycles.
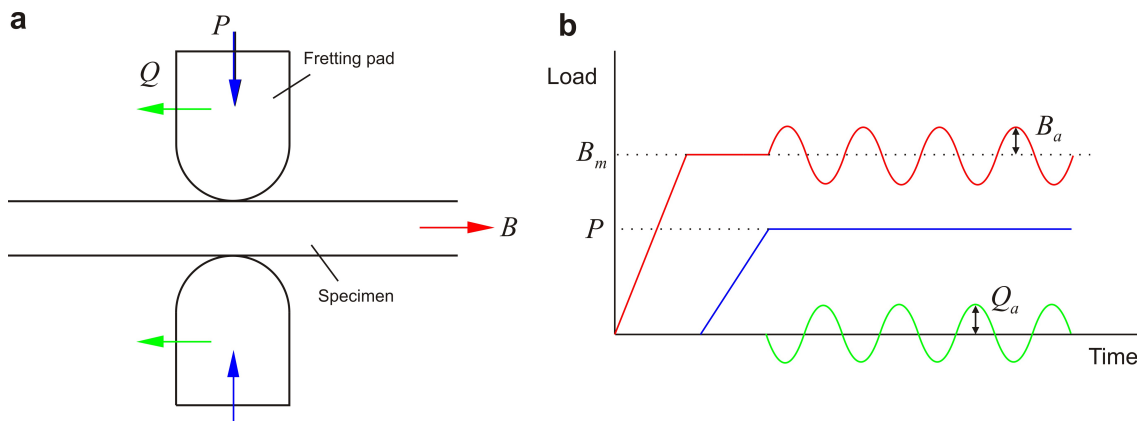
Figure 1. Fretting fatigue tests: Scheme (a) and loading program (b).

Table 3 lists the parameters and recorded lives of the fretting fatigue experiments where a is the contact semi-width, $\sigma_a = B_a/A$ is the bulk stress amplitude, p_o is the Hertzian peak pressure and Q_a is the tangential load amplitude. It is noted that as the mean bulk stress changes from tensile to compressive values the recorded life increases, and run out is reached for mean stresses less than -92.7 MPa. The results also show that fatigue endurance at 10^7 cycles is in the interval -92.7 MPa $\leq \sigma_m <$ -60 MPa. Figure 2 shows the post failure analysis of a run out test under a mean stress of -92.7 MPa. A cross section of the fretted zone along the length of the specimen was made by cutting and polishing the specimen. The existence of multiple cracks origins was observed. Initially, these cracks grew inclined to the bulk loading and then nearly perpendicular to it, before arresting.

3. MODELS FOR FRETTING FATIGUE ENDURANCE

3.1 Non-local multiaxial fatigue model

Non-local fatigue models have been applied in notches of mechanical components in order to take into account the stress gradient effect on fatigue strength. Taylor (1999) proposed a new framework for the formulation of non-local fatigue models called Theory of Critical Distances. In this approach fatigue endurance is governed by an average of the maximum principal stress over a volume element. Moreover, the size of the volume is a material parameter which is obtained with an identification procedure based on the threshold condition for crack propagation. In the same paper, models based on a line element or a point were also proposed.

Table 3. Parameters and results of fretting fatigue experiments.

a (mm)	σ_a(MPa)	p_o (MPa)	P (kN)	Q_a/P	f	σ_m (MPa)	Life (cycles)
1.19	92.7	350	8.5	0.25	0.54	15	164 662
1.19	92.7	350	8.5	0.25	0.54	15	202 609
1.19	92.7	350	8.5	0.25	0.54	0	198 686
1.19	92.7	350	8.5	0.25	0.54	0	274 248
1.19	92.7	350	8.5	0.25	0.54	-15	268 230
1.19	92.7	350	8.5	0.25	0.54	-15	299 568
1.19	92.7	350	8.5	0.25	0.54	-60	1 304 620
1.19	92.7	350	8.5	0.25	0.54	-60	1 552 276
1.19	92.7	350	8.5	0.25	0.54	-92.7	10 000 000
1.19	92.7	350	8.5	0.25	0.54	-145	10 000 000
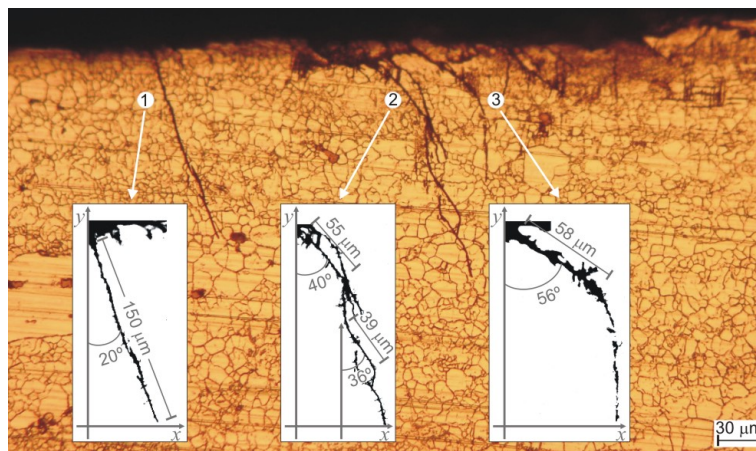
Figure 2. Post failure analysis of run out test under a mean stress of -92.7 MPa: Multiple crack origins and crack arrest.

Recent findings show that fretting fatigue endurance can also be addressed by non-local fatigue models originally proposed for sharp notches (Araújo (2007) and references therein). Accordingly, both fretting contacts and sharp notches produce steep stress distributions. Figure 3 shows the application of the non-local fatigue model assessed in this work to a plane contact under fretting fatigue:

$$\tau_a + \kappa \frac{\sigma_{n,max}}{\tau_a} - \lambda \leq 0, \quad \text{for all points where } y = 0.5L. \tag{1}$$

In this expression the critical plane fatigue model proposed in (Susmel and Lazzarin, 2002) is considered. Fatigue endurance will occur if the inequality is satisfied for all points at a depth $0.5L$ beneath the contact. The critical plane is defined as the material plane experiencing the maximum shear stress amplitude τ_a. The maximum normal stress upon the critical plane is denoted $\sigma_{n,max}$, while κ, λ and L are material parameters. The shear stress amplitude is defined as the radius of the minimum circumference enclosing the path described by the shear stress vectors on a material plane.

In order to identify the material parameters, three fatigue tests under threshold conditions are needed. For example, the parameters κ and λ can be identified by calibrating the fatigue model with the fully reversed and fluctuating tension fatigue limits of a plain specimen. This procedure gives:

$$\kappa = 0.5\tilde{\sigma}_a(\sigma_{-1} - \tilde{\sigma}_a)/\tilde{\sigma}_m, \quad \lambda = \kappa + 0.5\sigma_{-1}, \tag{2}$$

where σ_{-1} is the stress amplitude of a fully reversed test, and $\tilde{\sigma}_m$ and $\tilde{\sigma}_a$ are the mean and amplitude stress values of a fluctuating tension test, both under uniaxial and run out conditions. One strategy for the identification of L is to calibrate the fatigue model with the threshold condition for fatigue crack propagation under fully reversed loading (see Castro, 2008). This gives

$$L = \frac{1}{2\pi} \left(\frac{\Delta K_{th}}{\Delta \sigma_{-1}} \right)^2, \tag{3}$$

where ΔK_{th} is the threshold stress intensity factor range and $\Delta \sigma_{-1}$ is the uniaxial fatigue limit range, both under fully reversed loading.
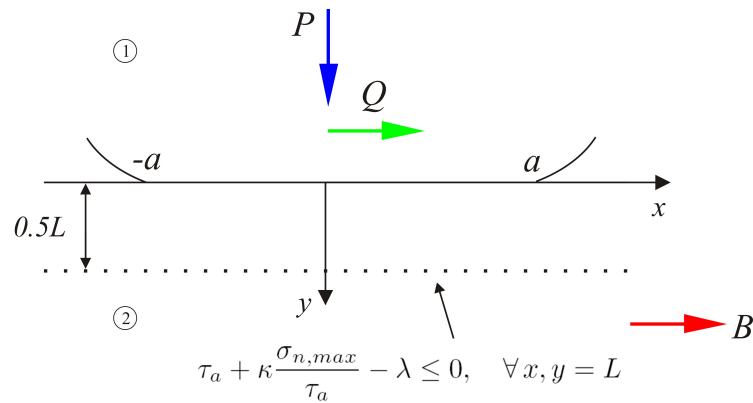
Figure 3. Application of the non-local fatigue model to a plane contact under fretting fatigue.

3.2 Crack arrest model

Fretting fatigue is characterized by steep stress gradients near the contact surface. In this context, cracks are greatly encouraged to initiate due to high stresses at the contact surface, but as they grow away from the surface their crack growth rate may become negligible. This is a safe condition always denominated crack self-arrest. Crack arrest models consider fatigue endurance of components under steep stress gradients as the limit condition for the existence of crack self-arrest. In this Subsection, following Araújo and Nowell (1999), a simple crack arrest model for fretting fatigue is proposed.

Figure 4a shows a scheme of the crack arrest model. A plane contact model between bodies 1 and 2 is considered. The most stressed point in the contact surface is assumed to occur at the trailing edge of the contact $(x, y) = (-a, 0)$ so that the crack origin is located in this vicinity. We also assume that the crack propagates normal to the surface. The crack depth is denoted b. The driving force for crack growth is evaluated by the Mode I stress intensity factor range, ΔK_I.

In the present context, fretting fatigue endurance is attained if

$$\Delta K_I(L) \leq \Delta K_{th}, \tag{4}$$

or

$$\exists b > L \mid \Delta K_I(b) = \Delta K_{th}, \tag{5}$$

where L is again given by expression (3). However, it is interpreted here as the minimum crack depth for which the assumptions of Linear Elastic Fracture Mechanics hold (Kitagawa and Takahashi, 1976). Condition (4) states that if the driving force ΔK_I at a depth L is below the threshold range for fatigue crack propagation, ΔK_{th}, then even if a crack has initiated its length will always be less than L. Expression (5) predicts that a propagating crack will arrest at a certain distance $b > L$ from the surface if its driving force, ΔK_I, becomes equal to ΔK_{th}. Figure 4b illustrates both conditions for fretting fatigue endurance as well as the condition for fatigue failure.

a

b
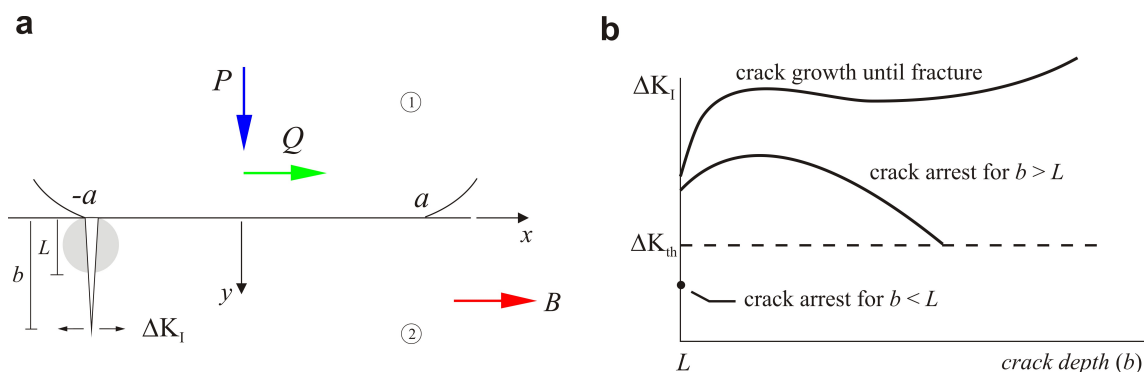
Figure 4. Scheme of the crack arrest model (a) and graph of the conditions for fatigue endurance and fatigue failure (b).

4. MODELS ASSESSMENT

In this section, we compare the predictions of the fretting fatigue endurance models with the experimental results for Al alloy 7050-T7451.

4.1 Elastic stress analysis

In order to apply the fretting fatigue models, first one needs to estimate the cyclic elastic stress distribution beneath the contact surface. In this setting, the experimental configuration was idealized as a plane contact model of a cylinder and a half-plane, both made of the same material. The contact pressure (normal traction) is given by the well-known elliptical Hertz distribution. The shear traction is similar to Mindlin–Cattaneo distribution except that the stick zone is shifted due to the alternating bulk stress in the specimen (Nowell and Hills, 1987). From the surface tractions, the subsurface stresses can be obtained via Muskhelishvili's potential (Hills and Nowell, 1994).

It is important to note that the analysis carried out by Nowell and Hills (1987) still holds in the present study, since in our loading program the specimen is first strained before being clamped. The only difference here is that a constant uniaxial mean stress has to be added in the stress field due to the initial straining of the specimen.

4.2 Results for the non-local multiaxial fatigue model

For the Al alloy 7050-T7451, the material parameters of the non-local multiaxial fatigue model were identified as: $\kappa = 18.8\,\mathrm{MPa}$, $\lambda = 92\,\mathrm{MPa}$ and $L \in [0.015\,\mathrm{mm}, 0.112\,\mathrm{mm}]$. The parameters κ and λ were obtained from expression (2) with the fully reversed fatigue limit given by $\sigma_{-1} = 146.6\,\mathrm{MPa}$, and the fatigue limit for a stress ratio $R = \sigma_{min}/\sigma_{max} = 0.08$ given by $\tilde{\sigma}_m = 120\,\mathrm{MPa}$ and $\tilde{\sigma}_a = 102.2\,\mathrm{MPa}$. Bounds for L were estimated from expression (3) by assuming that the threshold stress intensity range is such that $\Delta K_{\mathrm{th}} \in [2.0, 5.5]\,\mathrm{MPa}\sqrt{\mathrm{m}}$ based on typical values for Al alloys (Susmel et al., 2005).

Figure 5 shows the predictions of the non-local multiaxial fatigue model in a τ_a vs. $\sigma_{n,max}/\tau_a$ diagram. These results correspond to computations performed at the point $(x, y) = (-a, 0.5L)$, which is the critical one among all points at a distance $0.5L$ beneath the surface. The model is represented by a failure line which divides the diagram in a safe (below the line) and failure (above the line) domains, while each fretting fatigue test is represented by a point $(\sigma_{n,max}/\tau_a, \tau_a)$. It is worth noticing that τ_a was the same for all tests, while $\sigma_{n,max}/\tau_a$ varied. Indeed, the stress histories at $(x, y) = (-a, 0.5L)$ are the same in all tests, except for the value of the superimposed mean bulk stress. This produces only a shift of the shear stress path acting upon a material plane from test to test so that the radius of the minimum enclosing circumference is always the same. From the obtained results, we conclude that the model predicts complete failure of all specimens, while tests performed under mean stresses $-92.7\,\mathrm{MPa}$ and $-145\,\mathrm{MPa}$ ran out. A possible explanation for this behavior is that the non-local fatigue model is evaluated at a very small distance from the surface (here at $7.5\mu\mathrm{m}$ or $56\mu\mathrm{m}$) so that the influence of the high stress gradients has not yet disappeared. On the other hand, the non-local fatigue model correctly predicted crack initiation in all tests, since even in run out tests arrested cracks were observed (see Fig. 2).
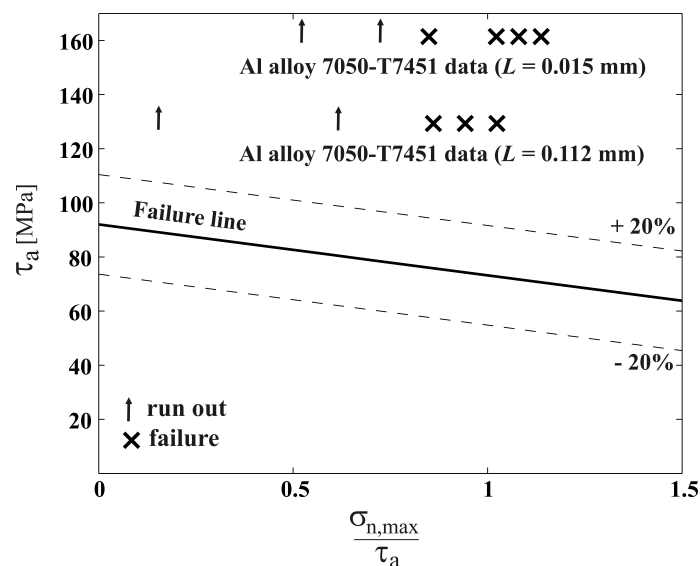
Figure 5. Predictions of the non-local multiaxial fatigue model.

4.3 Results for the crack arrest model

In order to implement the conditions for crack arrest expressed in (4) and (5), the stress intensity factor for a crack normal to the surface of a half-plane was obtained by the Distributed Dislocation Method (Hills and Nowell, 1994; Hills et

al., 1996). For a crack tip located at $(-a, b)$, the stress intensity factor range ΔK_I was evaluated as the difference between the maximum and minimum stress intensity factors along the loading history. Whenever the stress intensity factor was negative, it was set equal to zero. As in the previous Subsection, we assumed that the threshold stress intensity range, ΔK_{th}, for the Al alloy 7050-T7451 is in the interval $[2.0, 5.5] \, \mathrm{MPa}\sqrt{\mathrm{m}}$.

Figure 6 shows the variation of the stress intensity factor range with crack length for each fretting fatigue test. When the threshold stress intensity range is equal to $2.0 \, \mathrm{MPa}\sqrt{\mathrm{m}}$, then mean bulk stresses greater than -15 MPa produce crack propagation until fracture of the specimen. For mean bulk stresses less than -60 MPa, even if a crack is initiated its maximum length will be L, because at this length the stress intensity range is less than the threshold value for crack propagation. On the other hand, for a threshold stress intensity factor range equal to $5.5 \, \mathrm{MPa}\sqrt{\mathrm{m}}$ the model predicts fatigue endurance for all tests.
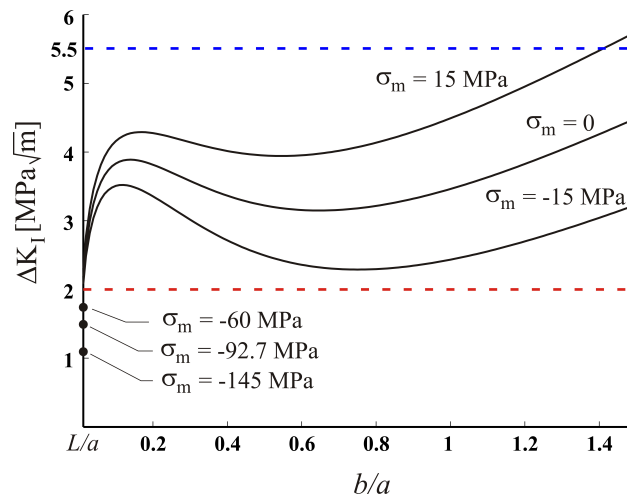
Figure 6. Variation of stress intensity factor range with crack length for each fretting fatigue test. Dashed lines represent thresholds for crack propagation.

5. CONCLUSIONS

In this work, an analysis of the mean stress effect on the fatigue endurance of a cylinder–flat contact configuration under partial slip conditions was carried out. Both fretting pads and specimens were manufactured from an Al alloy 7050-T7451 . Tests were conducted with identical contact tractions, but the mean bulk stress applied to the specimen varied from a compressive to a tractive value. Two fatigue models were proposed and compared with the experimental results: a non-local multiaxial fatigue model and a crack arrest model based on a mode I crack growth. The conclusions of this work are:

1. As the mean bulk stress changed from tensile to compressive values, the fretting fatigue lives increased. For run out tests, multiple crack origins were observed with subsequent crack arrest.

2. For the present fretting fatigue data, the non-local multiaxial fatigue model predicted complete failure of the two run out tests. On the other hand, it correctly predicted crack initiation in all tests.

3. The crack arrest model was able to predict both run out tests as well as complete failure (broken specimens). A more conclusive assessment was not possible since the threshold stress intensity range was estimated, not measured.

6. ACKNOWLEDGEMENTS

7. REFERENCES

Araújo, J.A. and Nowell, D., 1999, "Analysis of pad size effects in fretting fatigue using short crack arrest methodologies", International Journal of Fatigue, Vol.21, pp. 947-956.

Araújo, J.A., Susmel, L., Taylor, D., Ferro, J.C.T. and Mamiya, E.N., 2007, "On the use of the Theory of Critical Distances and the Modified Wöhler Curve Method to estimate fretting fatigue strength of cylindrical contacts", International Journal of Fatigue, Vol.29, pp. 95-107.

Araújo, J.A. and Castro, F.C., 2009, "Fadiga por Fretting: Caracterização e Aplicações Típicas", Metalurgia e Materiais, Vol.65, pp. 97-100.

Castro, F.C., Araújo, J.A. and Zouain, N., 2008, "On the application of multiaxial high-cycle fatigue criteria using the theory of critical distances", Engineering Fracture Mechanics, Vol.76(4), pp. 512-524.

Fouvry,S., Elleuch, K., Simeor, G., 2002, "Prediction of crack nucleation under partial slip conditions", Journal of Strain Analysis, Vol.37(6), pp. 549-564.

Fouvry,S., Nowell, D., Kubiak, K. and Hills, D.A., 2008, "Prediction of fretting crack propagation based on a short crack methodology", Engineering Fracture Mechanics, Vol.75(6), pp. 1605-1622.

Hills, D. and Nowell, D., 1994, "Mechanics of Fretting Fatigue", Kluwer Academic Publishers.

Hills, D., Kelly, P.A., Dai, D.N. and Korsunsky, A.M., 1996, "Solution of Crack Problems: The Distribution Dislocation Technique", Kluwer Academic Publishers.

Kitagawa, H. and Takahashi, S., 1976, In: Proceedings of the 2nd international conference on mechanical behaviour of materials, American Society for Metals, Philadelphia, pp. 627-631.

Nowell, D. and Hills, D., 1987, "Mechanics of fretting fatigue tests", Int. J. Mech. Sci., Vol.29(5), pp. 355-365.

Nowell, D., 1988, "An analysis of fretting fatigue", D. Phil. Thesis, Oxford University, 1988.

Susmel, L. and Lazzarin, P., 2002, "A bi-parametric Wöhler curve for high cycle multiaxial fatigue assessment", Fatigue and Fracture of Engineering Materials and Structures, Vol.25(1), pp. 63-78.

Susmel, L., Atzori, B., Meneghetti, G., 2005, "Material fatigue properties for assessing mechanical components weakened by notches and defects", Fatigue and Fracture of Engineering Materials and Structures, Vol.28, pp. 1-15.

Taylor, D., 2002, "Geometrical effects in fatigue: a unifying theoretical model ", International Journal of Fatigue, Vol.21(5), pp. 413-420.

8. Responsibility notice

The authors are the only responsible for the printed material included in this paper.